AJNR

Origin of Synchronized Low-Frequency Blood Oxygen Level–Dependent Fluctuations in the Primary Visual Cortex

J.S. Anderson

AJNR Am J Neuroradiol 2008, 29 (9) 1722-1729
doi: https://doi.org/10.3174/ajnr.A1220
http://www.ajnr.org/content/29/9/1722

ORIGINAL RESEARCH

Origin of Synchronized Low-Frequency Blood Oxygen Level–Dependent Fluctuations in the Primary Visual Cortex

J.S. Anderson

BACKGROUND AND PURPOSE: Low-frequency (<0.08 Hz) fluctuations in spontaneous blood oxygen level–dependent (BOLD) signal intensity show synchronization across anatomically interconnected and functionally specific brain regions, suggesting a neural origin of fluctuations. To determine the mechanism by which high-frequency neural activity results in low-frequency BOLD fluctuations, I obtained measurements of the effects of neurovascular coupling on the frequency content of BOLD fluctuations.

MATERIALS AND METHODS: 3T recordings of BOLD signal intensity in the primary visual cortex were obtained in response to visual stimuli presented at varying temporal frequencies to determine which stimulus frequencies were successfully transmitted to BOLD signal intensity. Additional BOLD time series recordings were performed in a resting state and during natural visual stimulation, and frequencies comprising BOLD fluctuations were measured. Magnetoencephalographic (MEG) time series recordings were obtained in a resting state to measure which components of MEG signal intensity best correlated in frequency distribution to observed BOLD fluctuations.

RESULTS: Visually driven oscillations in BOLD signal intensity were observed up to 0.2 Hz, representing a mismatch between low-pass filter properties of neurovascular coupling and observed frequencies of spontaneous BOLD fluctuations, which are <0.05 Hz in the primary visual cortex. Visual stimulation frequencies of >0.2 Hz resulted in frequency-dependent increases in mean BOLD response. Amplitude modulation of high-frequency neural activity was measured in MEG time series data, which demonstrated 1/frequency distribution with the greatest power comprising frequencies <0.05 Hz, consistent with the distribution of observed BOLD fluctuations.

CONCLUSION: Synchronized low-frequency BOLD fluctuations likely arise from a combination of vascular low-pass filtering and low-frequency amplitude modulation of neural activity.

Since the discovery of synchronized low-frequency (<0.08 Hz) fluctuations in blood oxygen level–dependent (BOLD) signal intensity among functionally related brain regions,[1] the application of functional MR imaging (fMRI) to studying functional connectivity has led to increasing interest in identifying the physiologic source of these fluctuations. Early speculation about the technique questioned the possibility that fluctuations might be generated by artifacts such as aliasing of cardiac or respiratory pulsations in the low-frequency range, vasomotor oscillations, or effects of attention.[2]

Subsequent investigations now provide strong evidence that synchronous low-frequency fluctuations have a neural source. First, time series measurements of BOLD signal intensity at a high temporal frequency (TR = 400 ms) showed only minimal components of the BOLD signal intensity at cardiac and respiratory frequencies in recordings from several cortical regions.[3] Subsequent analysis of respiration artifact showed significant artifact only in regions of prominent vessels such as the circle of Willis.[4]

Second, a growing literature has demonstrated high functional specificity of networks exhibiting synchronized BOLD fluctuations. Resting (no task) recordings have convincingly delineated synchronized networks that are intrinsically active in the absence of a task,[5-7] with anatomic boundaries corroborated from studies using a wide range of tasks by means of fMRI, positron-emission tomography, and electroencephalographic (EEG) techniques.[8-10] Other reports have shown synchronized networks involving precisely those regions known to be involved in visual, auditory, and language function.[11,12] Subcortical networks involved in memory[13] and thalamo-hippocampal[14] circuits also showed loci of synchrony that corresponded to known neuroanatomic pathways. Large-scale analyses have demonstrated the functionally organized topology of synchronized networks.[15]

Third, networks with synchronized BOLD fluctuations have shown coherent modulation with behavior and alteration in numerous pathologic states. Direct recording from the primary auditory cortex in neurosurgical patients has demonstrated tight correlation between BOLD fluctuations and separately acquired local field potentials, phase-locked to a common stimulus.[16] Brain regions involved in episodic memory function have shown increased synchrony during performance of a memory-encoding task.[17] In a button-pressing task, a large fraction of the trial-to-trial variability in BOLD response was accounted for by synchronized fluctuations.[18] Differences in amplitude of low-frequency oscillations have been observed between eyes-open and eyes-closed conditions.[19] Alteration in synchrony of spontaneous BOLD fluctuations have been observed in autism,[20,21] Alzheimer disease,[22] mild cognitive impairment,[23] multiple sclerosis,[24]

Received April 14, 2008; accepted after revision May 27.

From the Department of Neuroradiology, University of Utah, Salt Lake City, Utah.

This work was supported by the Benning Foundation.

Paper previously presented at: Annual Meeting of the American Society of Functional Neuroradiology, May 31–June 5, 2008; New Orleans, La.

Please address correspondence to Jeffrey S. Anderson, 1A71 SOM, University Hospital, Salt Lake City, UT 84132; e-mail: andersonjeffs@gmail.com

DOI 10.3174/ajnr.A1220

blindness,[25] schizophrenia,[26] and agenesis of the corpus callosum.[27]

Yet, the mechanism by which neural activity results in BOLD fluctuations that are orders of magnitude slower than the underlying neural activity is not understood. Measurement of frequencies contributing to synchronized BOLD activity have shown distribution in which nearly all of the power in the fluctuations arises from frequencies of <0.08 Hz.[3,28]

To evaluate what mechanisms might contribute to low-frequency BOLD fluctuations, I recorded fMRI time series data at a high temporal frequency in the primary visual cortex in response to visual stimuli presented at prescribed frequencies to measure the temporal structure of neurovascular coupling. Subsequently, magnetoencephalographic (MEG) recordings of the occipital lobes were obtained to evaluate the temporal relationship between spontaneous MEG activity and BOLD fluctuations.

Materials and Methods

Subject Characteristics

Experimental procedures were approved by the University of Utah institutional review board. Informed consent was obtained for all subjects. 3T fMRI recordings were obtained from 19 healthy volunteer subjects (16 men, 3 women; average age, 29.5 ± 3.6). All fMRI subjects were fitted with MR imaging–compatible lenses to allow comfortable reading of the 8-point text within the scanner. An additional 6 volunteers (5 men, 1 woman; average age, 35.3 ± 6.2) were then studied with MEG, described below.

fMRI Acquisition

Images were acquired on a 3T Trio scanner (Siemens, Erlangen, Germany). Subject monitoring was performed throughout the examination by real-time eye tracking by using an infrared camera mounted on a 12-channel head coil. Scanning protocol consisted of an initial 2-mm isotropic magnetization-prepared rapid acquisition of gradient echo (MPRAGE) acquisition for the anatomic template. A field map sequence was acquired for off-line distortion and magnetic inhomogeneity correction. BOLD echo-planar images (TR = 1 second, TE = 28 ms, generalized autocalibrating partially parallel acquisition [GRAPPA] with an acceleration factor of 2, 11 sections at 3-mm section thickness) were obtained for 4 minutes during presentation of a flashing checkerboard stimulus shown to alternating left and right hemifields in 20-second intervals with a block design. Motion correction was performed during BOLD imaging with a prospective acquisition-correction technique sequence.

On-line thresholding was performed in real time by using a general linear model with Neuro3D software (Siemens) to obtain activation maps. Three- or 5-section regions in an oblique axial plane including the pericalcarine primary visual cortex and either the lateral geniculate nuclei (LGNs) or the frontal eye field foci of activation were selected for all subsequent BOLD series, and additional 4-minute acquisitions with the same visual stimuli were performed to use as a template for visual regions of interest in off-line postprocessing. Subsequent BOLD series used the same sections and protocol (3 or 5 sections, 3-mm section thickness, 64 × 64 matrix with in-plane resolution of 3 × 3 mm, TR = 200 ms for 3 sections in 8 subjects, TR = 300 ms for 5 sections in 11 subjects, TE = 28 ms to central *k*-space, GRAPPA = 2).

Nineteen subjects then were assigned 1 of 3 protocols. In 6 subjects, 14-minute BOLD acquisitions were performed in a resting state condition (eyes closed, subjects instructed to "remain awake and let thoughts pass through their mind without focusing on any one thought") and then during natural visual stimulation (Bugs Bunny cartoon, Looney Tunes).

In 7 subjects (data from 1 subject were discarded because of an inability to remain awake through the examination), visual stimuli were flashed for a single screen refresh on an LCD projector at several prescribed frequencies. Each run consisted of a single frequency condition with a 7-minute duration. Between 4 and 6 runs were performed per subject.

In 6 subjects, visual stimuli were flashed at 6 Hz during ON periods and an isoluminant gray screen was displayed with a central fixation spot during OFF periods. ON and OFF periods alternated at multiple frequencies (from the start of the ON period to the start of next ON period). Each frequency condition lasted for 1 minute, and 7 conditions were presented in pseudorandom order during 1 run. Each subject was shown the same frequency conditions in varying order between 4 and 6 runs. A total of 9 frequencies were shown to the subjects (not all frequency conditions were shown to all subjects.)

Stimulus Presentation

Visual stimuli were generated with custom-designed software by using the Psychophysics Toolbox[29] platform for Matlab (MathWorks, Natick, Mass). A stimulus-presentation computer was synchronized with the scanner by acquisition of an optical pulse emitted by the scanner at the start of each BOLD sequence via an optic-electric converter and a digital acquisition board.

Stimuli were displayed on an LCD projector with a luminous RE-6011 shutter (Avotec, Stuart, Fla), and submillisecond accuracy was confirmed with use of a photometer and oscilloscope. All presentation data were logged with a frame-by-frame audit at the level of each screen refresh.

Stimuli were viewed on an 8-inch screen mounted in the bore of the scanner approximately 6 inches from the patient's eyes and viewed by a mirror mounted on the top of the head coil. All subjects were fitted with magnetically inert goggles with appropriate vision corrective lenses.

fMRI Postprocessing

Off-line postprocessing was performed in Matlab (MathWorks) by using SPM5 toolbox with MarsBaR toolbox extension.[30] A field map sequence was used for distortion correction, and all images were motion corrected by using a realign and unwarp procedure. BOLD images were then coregistered to the MPRAGE anatomic image sequence. No image normalization or smoothing was performed.

Activation maps were generated from dedicated 4-minute visual stimulation (Fig 1) BOLD data by using a general linear model (false discovery rate, $P = .005$). Regions of interest corresponding to the primary (pericalcarine) visual cortex, extrastriate visual cortex, LGN, and frontal eye fields were obtained for each subject by selecting the dominant cluster in each region. This technique allowed voxel selection independent of frequency conditions in subsequent BOLD acquisitions.

Time series were extracted with the MarsBaR toolbox for each region of interest by using average data across the region of interest for each BOLD sequence obtained in that subject. Time series data were processed by linear detrend to correct for scanner drift. Averaging for

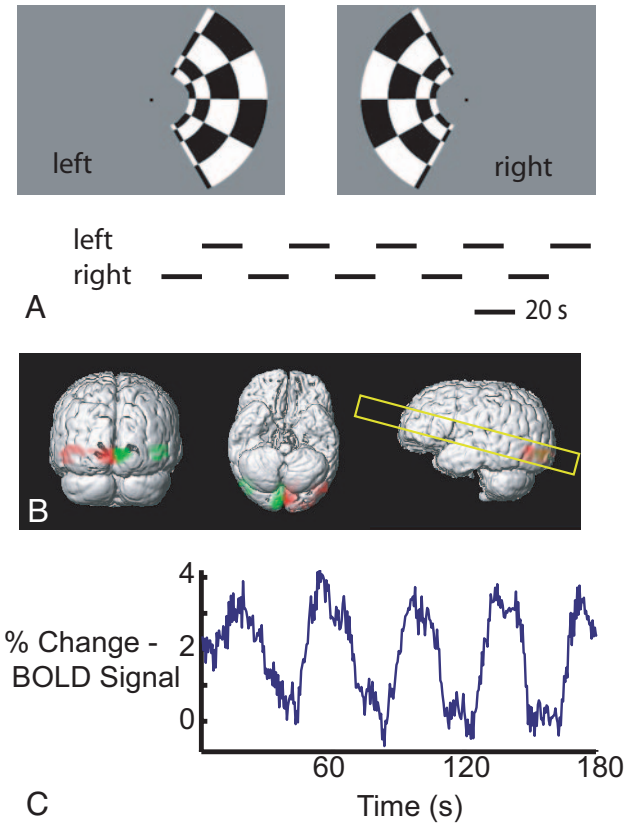

Fig 1. Selection of regions of interest. *A,* Visual stimuli shown to right and left hemifields corresponding to activation in left and right visual cortices. Stimuli were flashed with alternating black and white regions (100% contrast) at 6 Hz, alternating between left and right images every 20 seconds for 4 minutes. *B,* Activation maps in 1 subject from previously mentioned stimulation. Activation in the primary and extrastriate visual cortex is seen on the left in red and on the right in green. The yellow box on the sagittal view shows the brain region acquired for BOLD sequences. *C,* Left visual cortex time series. Slightly >3% increase in BOLD signal intensity is seen averaged across the left primary visual cortex cluster. Three minutes of data are shown.

each frequency condition and power spectral analysis was performed with custom-designed software for the Matlab platform.

The resting fMRI time series data were extracted from the visual cortical, LGN, and frontal eye field clusters described previously by using MarsBaR toolbox. A linear detrend function was used to correct for scanner drift over each 14-minute acquisition. Power spectral analysis was performed with Time Series Tool software in Matlab.

MEG Analysis

MEG data were collected by using a Neuromag (Elekta Instruments, Stockholm, Sweden) whole-head system with 306 MEG sensors comprising 102 magnetometers and 204 gradiometers. The MEG sensor elements are in 102 locations. There are 2 orthogonally placed planar gradiometers and 1 magnetometer at each sensor location. The Elekta Neuromag whole-head MEG system has a single dewar, and the sensors are immersed in liquid helium to keep the SQUIDS in cryogenic temperature. The MEG system is located in a 2-layered magnetically shielded room. The data were collected with a sampling rate of 600 Hz and a high-pass filter of 0.01Hz, with a 32-bit resolution.

Six subjects were studied with MEG, consisting of a 10-minute recording with their eyes closed. Subjects were instructed to remain awake and to try to clear their minds, letting thoughts pass through rather than focusing on any 1 mental activity. A gradiometer overlying the left occipital pole was selected for each patient, and raw time series data were extracted.

Raw data were then bandpass-filtered in Matlab with the Time Series Tool by using the Ideal Pass Filter in δ, α, β, and γ ranges. Data were then full-wave rectified, and the envelope function was computed by replacing each point in the time series by the maximal value of the time series within 1 period corresponding to the lower bound of the bandpass frequency range. Thus, for the α range filter (8–13 Hz), the sliding maximal function with a 125-ms window (corresponding to 8 Hz) was used to calculate the envelope function. Power spectral analysis was performed with the Time Series Tool in Matlab.

Results

Synchrony between Functionally Related Brain Regions

In 6 subjects, BOLD time series data in a resting state (eyes closed, no task) and during natural visual stimulation were acquired for 14 consecutive minutes each. From these subjects, statistically significant clusters were seen in postprocessed images in the LGN in 3 subjects, in the frontal eye fields in 2 subjects, and in the primary visual cortex and extrastriate visual cortex in all subjects.

The contralateral primary visual cortices showed highly synchronous BOLD fluctuations (Fig 2) in all subjects. Synchrony was also observed between the visual cortex and the LGNs (Fig 2*C*) in each of the subjects measured. Synchrony between the bilateral frontal eye fields was seen with a slower time course, indicated by a broad slow peak on the cross-correlation plot in 1 subject and a smaller narrower peak in the other subject (Fig 2*C*). The very slow cross-correlation peak in frontal eye fields in 1 subject was distinctly different from the correlation observed in other visual areas, and it is possible that this represents an artifactual physiologic signal intensity such as from eye movements during the acquisition.

Effect of Neurovascular Coupling on the BOLD Response

In 13 subjects, BOLD responses in the primary visual cortex were recorded to flashing visual stimuli presented at varying frequencies. Two separate stimulation paradigms were used. In the first paradigm (6 subjects, Fig 3*A* right), radial checkerboard stimuli were flashed to the bilateral visual field for a single screen refresh (13 ms) at 6 frequencies ranging from 0.1 Hz to 4 Hz.

In the remaining 6 subjects (Fig 3*A* left), a 6-Hz flashing checkerboard stimulus was alternated ON and OFF at several of 9 frequencies ranging from 0.017 to 0.5 Hz. In this paradigm, the same total number of flashes of the stimulus was constant for every frequency condition.

For both stimulation paradigms, the F1(peak-to-peak amplitude) component of the driving stimulus was preserved in the BOLD responses for frequencies up to approximately 0.15 Hz, beyond which there was a gradual decline in peak-to-peak amplitude between 0.15 and 0.3 Hz (Fig 3*B*). Although 2 separate paradigms were used, 1 with weak stimuli and 1 with strong stimuli, virtually identical measurements of filter properties of neurovascular coupling were observed in the frequency range over which both paradigms overlapped.

Also for both stimulation paradigms, there was a uniform increase in mean BOLD signal intensity with increasing stim-

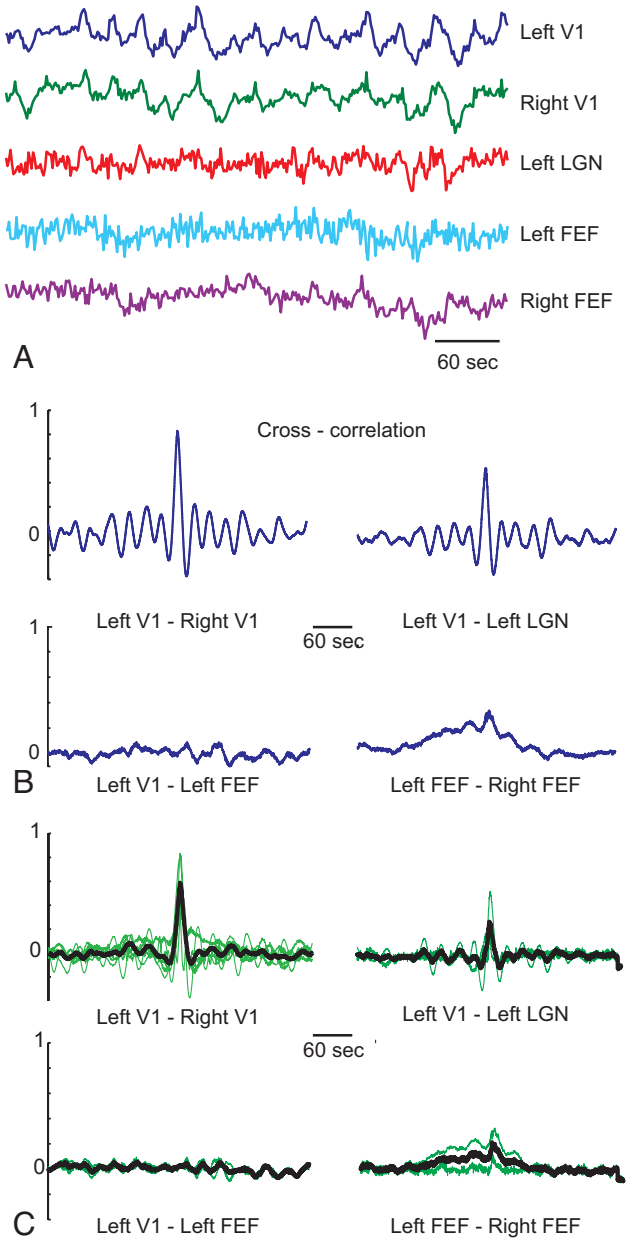

Fig 2. Synchronized BOLD fluctuations. *A*, Time series data from 1 subject. Six minutes of data are shown. Traces represent average BOLD signal intensity from regions of interest in the bilateral primary visual cortex (V1), left LGN, and bilateral frontal eye fields (FEF). *B*, Cross-correlation analysis represents full 14-minute resting state data from regions listed previously. Bilateral V1 shows strong focal correlation, with similar but diminished correlation between V1 and LGN. No correlation is seen between V1 and FEF. Bilateral FEF show much broader temporal correlation. *C*, Summary resting state BOLD cross-correlation from 6 subjects. Green traces show cross-correlograms for individual subjects, and black traces show an average cross-correlogram across subjects (bilateral V1, $n = 6$; left V1-left LGN, $n = 3$; left V1-left FEF, $n = 2$, left FEF-right FEF: $n = 2$).

ulus frequency (Fig 3*C*), observed even in the paradigm for which the total number of stimulus presentations was constant for each frequency condition. This suggests that periods of higher frequency neural activity than can be reproduced in BOLD fluctuations (ie, >0.2 Hz) may be transmitted as an increased mean BOLD response. If such high-frequency activity was modulated in amplitude or frequency at relatively slow rates, these data would imply that the resulting BOLD response may show a resulting slow fluctuation.

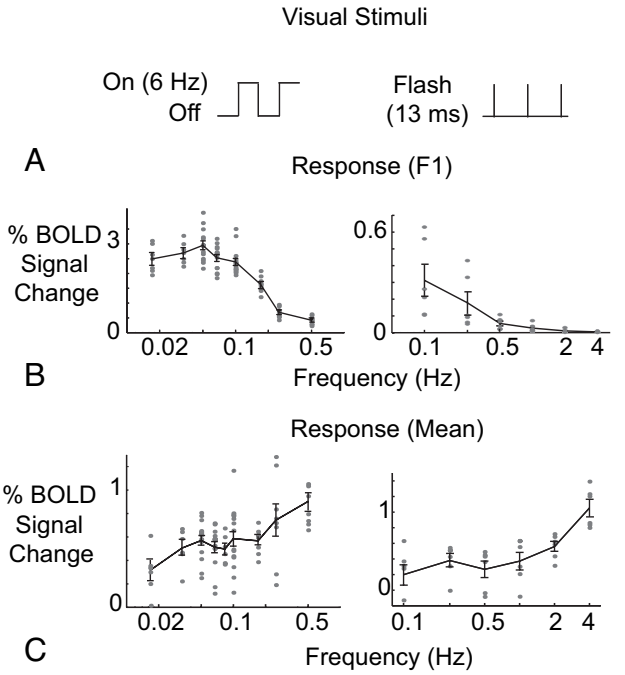

Fig 3. Vascular low-pass filtering of neurovascular coupling. *A*, Data in the first column represent BOLD responses to a 6-Hz flashing radial checkerboard pattern turned ON and OFF at frequencies ranging from 0.01 to 0.5 Hz. Data in the second column represent BOLD responses to single flashes of 1 screen refresh duration (13 ms) of the same radial checkerboard pattern presented at frequencies ranging from 0.1 to 4 Hz. *B*, Peak-to-peak response for 1 period of the stimulus. Individual points plotted are responses from each subject of the amplitude of the BOLD response averaged across all cycles of stimulus presentation. Left and right hemifield responses are plotted as separate data points on the left and are averaged for each data point on the right. Error bars represent 1 standard error of the mean. *C*, Mean BOLD responses compared with baseline (blank screen stimulus), averaged across the entire trial for each frequency condition. Data points and error bars are as in Fig 3*B*.

Frequency Components of BOLD Fluctuations

Power spectra were obtained to analyze frequencies present in the spontaneous (eyes closed) BOLD fluctuations from the initial 6 subjects, normalized and averaged across the 6 subjects (Fig 4*A*). None of the subjects exhibited any significant contribution in visual cortical BOLD time series data from frequencies attributable to cardiac (~1 Hz) or respiratory (~0.2 Hz) pulsations, similar to observations by Cordes et al.[3] Rather, virtually the entire power distribution of the BOLD fluctuations was concentrated at frequencies <0.05 Hz. When these frequencies are compared with low-pass filter properties observed in Fig 3 from which stimulus frequencies (and presumably frequencies of neural activity) are successfully transmitted to BOLD signal intensity, there is a mismatch. Frequencies between 0.05 and 0.15 Hz are virtually absent from BOLD fluctuations (Fig 4*B*).

Comparing power spectra from the BOLD time series obtained in the eyes-closed condition with the natural visual stimulation condition shows higher frequencies in the eyes-closed condition (Fig 5). Average power was calculated between 0 and 0.02 Hz ($P < .02$) and between 0.02 and 0.05 Hz ($P < .03$) for each subject. A pair-wise 2-tailed t test ($n = 6$) demonstrated statistical significance between the 2 conditions in each frequency range (Fig 5). The difference between conditions would be consistent with the hypothesis that frequency distribution of BOLD fluctuations is influenced by underlying

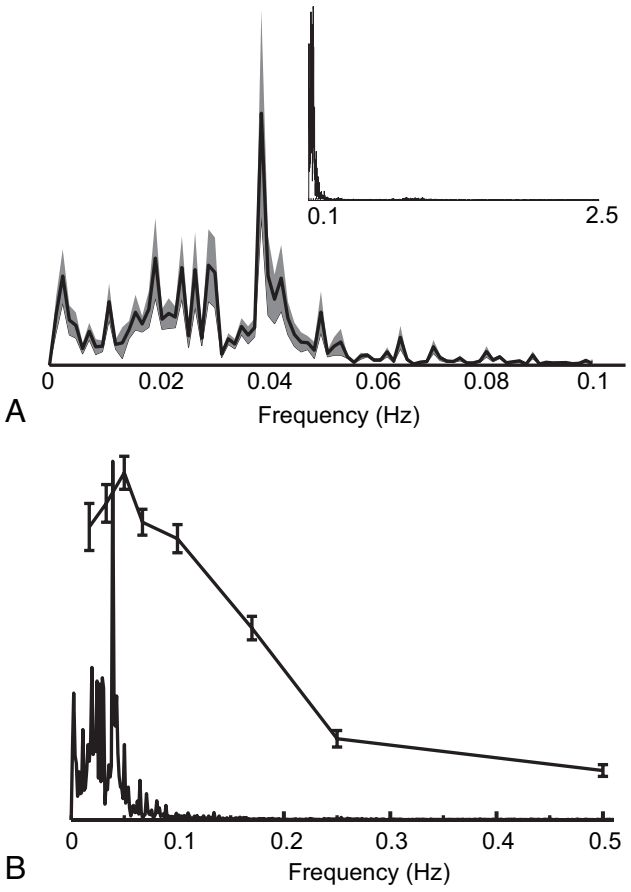

Fig 4. Frequencies present in spontaneous BOLD fluctuations in the primary visual cortex. *A,* Full-field (inset) and zoomed-in power spectra of resting-state BOLD fluctuations. Spectra are computed for each subject, normalized to the unit area under the curve, and averaged across subjects. Shaded regions represent ±1 standard error of the mean as a function of frequency. *B,* Superimposed vascular filtering data of Fig 3*B* and the resting-state power spectrum from Fig 4*A*. Frequencies between 0.05 and 0.2 Hz are underrepresented if frequency distribution of spontaneous BOLD fluctuations arises from vascular filtering alone.

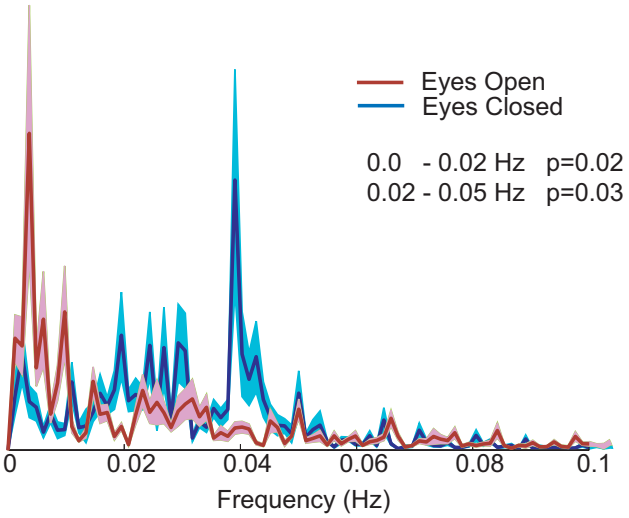

Fig 5. Power in spontaneous BOLD fluctuations in resting and visual stimulation conditions. Resting state (blue) condition shows the shift of frequency distribution to higher frequencies compared with natural visual stimulation condition (red). Spectra are averaged across 6 subjects for each condition. Shaded areas represent standard error of the mean as a function of frequency across the population. The pair-wise *t* test for each frequency range (0–0.02 Hz and 0.02–0.05 Hz) indicates statistically significant differences between the 2 conditions for each of the 2 ranges.

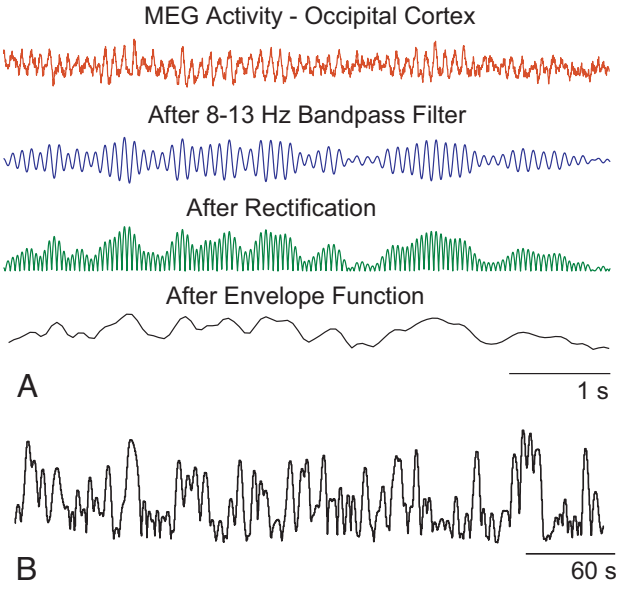

Fig 6. Amplitude modulation of MEG signal intensity. *A,* Procedure for calculating amplitude modulation for each frequency band of the MEG signal intensity. Raw data were first bandpass-filtered into δ, α, β, and γ bands. Data were then full-wave-rectified, and an envelope function was calculated to measure the variation in amplitude with time. Approximately 5 seconds of data are shown. *B,* Envelope function from Fig 6*A* for 1 subject. Approximately 7 minutes of data are shown. Note the similarity in appearance of low-frequency fluctuations to BOLD fluctuations shown in Fig 2.

neural activity and that fluctuations do not merely represent correlated physiologic noise.

Amplitude Modulation of Neural Activity

To evaluate whether underlying neural activity may show slow modulation at frequencies likely to contribute to the observed low-frequency BOLD fluctuations, I studied an additional 6 subjects with MEG recordings in the eyes-closed condition.

Processing of MEG data is illustrated in Fig 6. Raw data from the occipital gradiometer were first bandpass-filtered into each of the δ, α, β, and γ bands, and the mean value of the data was subtracted. Each trace was then full-wave rectified,[31] and the envelope function was calculated. The resulting amplitude modulation curve of α activity for 1 subject is illustrated with accompanying power spectrum in Fig 6.

MEG data were obtained in the eyes-closed condition, and the full-range power spectrum of the data was dominated by α activity, as might be expected for an occipital recording (Fig 7*A*). For this subject, the power spectrum of the envelope function for α filtered activity matches precisely a 1/frequency curve (Fig 7*B*).

Summary data for each of the frequency bands measured are presented in Fig 7*C–F*. All bands show very high power at low frequencies, with curves approximating scaled versions of 1/frequency, though frequency bands show variable rates of decay in power with increasing frequency. For all frequency bands, there is a striking increase in power at frequencies below ~0.05 Hz.

Discussion

An accurate understanding of the mechanism whereby spontaneous neural activity translates to much lower frequency

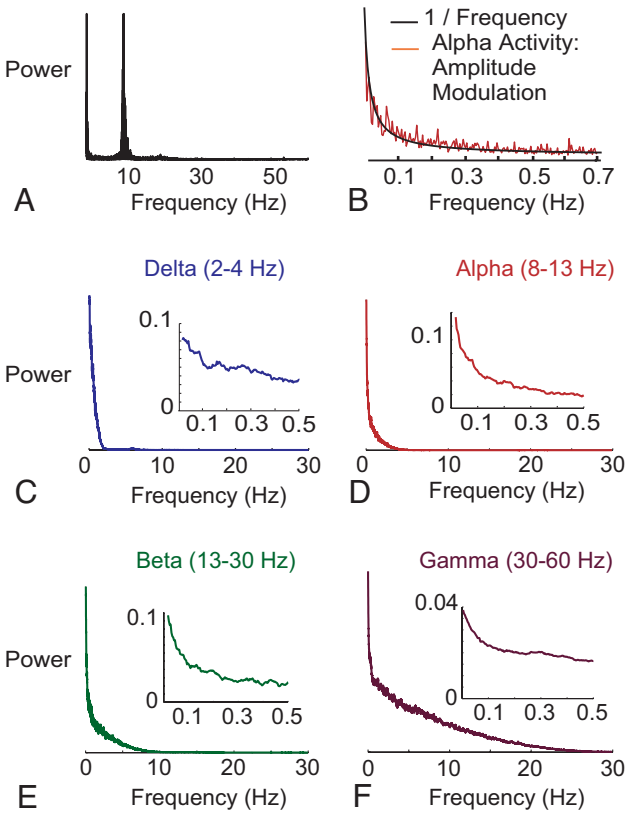

Fig 7. The 1/frequency distribution of amplitude modulation of MEG signal intensity. *A*, Full-field power spectrum of unfiltered MEG signal intensity in 1 subject, resting state. Note that most of the power comprises α activity. *B*, The power spectrum for amplitude modulation of α activity from data in Fig 6*B*. A 1/frequency curve shows excellent fit to the data. *C*, Amplitude modulation of δ activity. Full-field power spectrum with inset showing zoomed-in region of the curve up through 0.5 Hz. Data show averages from normalized power spectra from 6 subjects. *D–F*, As per Fig 7*C* for α, β, and γ activity, also averaged from 6 subjects.

BOLD fluctuations is increasingly important as techniques using these synchronized fluctuations are being applied to a wide range of pathologic conditions.[17-24] In particular, it would be useful to know whether synchronized fluctuations reflect correlated neural noise or whether there is neurophysiologic information accessible within the temporal structure of the fluctuations.

Data presented here indicate that a large part of the mechanism responsible for translation of neural activity to BOLD signal intensity is mediated by filter properties of neurovascular coupling. Low-pass filtering is demonstrated to restrict transmission of oscillations at frequencies of >0.3 Hz and results in increasing damping of frequencies between 0.1 and 0.3 Hz.

Yet neurovascular coupling alone is unlikely to explain the frequency distribution of observed BOLD fluctuations, in which frequencies ≤0.05 Hz are actively represented, but frequencies between 0.05 and 0.2 Hz are not represented to the extent expected by filtering alone. From these data, it is expected that some other mechanism contributes to the observed frequency range of spontaneous BOLD fluctuations. Although low-frequency fluctuations have traditionally been described as <0.08 Hz,[27] the visual cortical fluctuations observed in this report were almost exclusively <0.05 Hz.

A contribution of high-frequency neural activity to synchrony in BOLD signal intensity, and not merely of low-frequency filtered components or harmonics of the neural activity, is also suggested from several other reports. Examination of local field potential (LFP) in the monkey visual cortex demonstrated that though synchrony in the raw LFP diminished rapidly with cortical distance, band-limited power in the γ frequency range showed synchrony over much larger cortical distances.[29] In a simultaneous measurement of LFP and optical hemodynamic response, there was tight correlation of power of local field potential oscillations in the γ range with hemodynamic response.[32] Gamma-range LFP and BOLD responses showed high temporal correlation and coincided with periods of synchrony among interneurons, in a study measuring individual unit activity, LFP, and BOLD response.[33]

Other reports have also shown correlation between low-frequency synchronized BOLD fluctuations and other ranges of higher frequency neural activity. An investigation of simultaneous EEG and fMRI revealed a correlation between BOLD fluctuations and power in δ, θ, α, β, and γ ranges, with variable contributions in different spatially separated distributed networks.[34] An analysis of resting-state networks by using epidural EEG and fMRI in anesthetized rats showed the highest correlation between the δ range power in the contralateral somatosensory cortex.[35] Higher frequency ranges have also been shown to be dependent, with coupling between γ and è oscillations in 1 study,[36] supporting the idea of distributed synchrony among temporal frequency ranges.

One possibility for generating slow fluctuations in hemodynamic responses is infrequent high-amplitude epochs of spontaneous neural activity, or neural avalanches.[37] Temporal inhomogeneity of spontaneous neural activity is well described. Many neocortical neurons exhibit, for example, slow 2-state fluctuations in membrane potential and spiking rates.[38] Such fluctuations participate in sensory-information encoding[39] and are synchronized over wide cortical networks.[40] Discrete states at slow time scales among more distributed neural networks have also been proposed as a mechanism for neural computation.[41]

Yet analysis of time series data in BOLD and MEG responses does not show discrete periods of activity followed by relative inactivity but shows continuous slow fluctuations with somewhat variable frequency and amplitude within a narrow range. Thus, temporal inhomogeneity may contribute to low-frequency fluctuations, but data appear more consistent with a slow modulation of frequency and amplitude of neural activity than infrequent, salient, and discrete periods of activity.

The data previously mentioned demonstrate that at frequencies of >0.3 Hz, increasing frequencies of presented stimuli (and neural activity) are transmitted as increased mean BOLD signal intensity, suggesting that slow modulation in the time of the BOLD signal intensity could be produced by a similar modulation in the time of frequency or amplitude of neural activity. MEG data confirm that such slow modulation in the amplitude of given frequencies is indeed present. Moreover, across all frequency bands, envelope functions of amplitude modulation demonstrate 1/frequency distribution, with the greatest power below 0.05 Hz.

Such modulations would be an excellent candidate for amplification of very low frequencies seen in BOLD fluctuations.

They would preserve synchrony of high-frequency power that other studies have shown to be correlated to BOLD low-frequency synchrony and could explain the mismatch between low-pass-filter properties of neurovascular coupling shown previously and observed BOLD frequency distribution.

The 1/frequency distribution seen in amplitude modulation of neural activity is a pervasive property of numerous physical systems, ranging from light emission by quasars to flow through rivers and current flow through resistors,[42] and is seen extensively in biologic systems including fMRI time series data.[43] The presence of 1/frequency distribution in the modulation of the band-limited amplitude of neural activity suggests that this modulation is generated by a stochastic process, though this does not exclude the possibility that parameters of the noise may reflect static or dynamic properties of the neural system.

The data in this report are drawn from different populations of volunteers, in particular the subjects from whom fMRI and MEG data were obtained. It might strengthen the agreement in frequency distribution between the MEG amplitude modulation data and the fMRI time series data presented previously if the results had been drawn from the same population. Yet the frequency ranges observed in visual cortical fMRI time series are remarkably consistent with those reported in other studies,[3] and observing similar results for frequency ranges of resting state data across multiple modalities, subject populations, and experimental designs strengthens the argument that amplitude modulation of neural activity produces frequency distribution that is conserved across subjects.

Conclusion

Synchronized BOLD fluctuations in the primary visual cortex comprised frequencies of <0.05 Hz, but visual stimulation with frequencies ≤ 0.2 Hz can drive oscillations in the BOLD signal intensity. Therefore, although low-pass filtering from neurovascular coupling likely makes a large contribution to the frequency components observed in BOLD fluctuations, it is insufficient to explain the observed frequencies by itself. Amplitude modulation of neural activity appears to occur at predominantly low frequencies, with the greatest power <0.05 Hz and 1/frequency distribution. Such changes in amplitude of neural activity are likely reflected in the BOLD response by a slow fluctuation and would be an ideal component for amplification of very low frequencies in the BOLD response. Amplitude modulation, together with vascular low-pass filtering, could provide a mechanism for the observed frequency distribution of spontaneous BOLD fluctuations.

If synchronized BOLD fluctuations, which have been shown to correlate with neural responses, brain pathology, and functional connectivity, are generated at least in part from amplitude modulation of epochs of synchronized high-frequency neural activity, then the implication that information may be encoded in such low-frequency modulation suggests a target to explore in future studies. Moreover, because the distribution of low frequencies of BOLD fluctuations was altered with visual stimulation, the timing of amplitude modulation of neural activity may represent a useful metric of regional connectivity that could be used in neurophysiologic and pathologic investigations.

Acknowledgments

I thank James N. Lee for technical suggestions on simultaneous fMRI acquisition of LGN and the primary visual cortex regions and Michael Funke and Pegah Afra for assistance with MEG acquisition.

References

1. Biswal B, Yetkin FZ, Haughton VM, et al. **Functional connectivity in the motor cortex of resting human brain using echo-planar MRI.** *Mag Res Med* 1995;34:537–41
2. Maldjian JA. **Functional connectivity MR imaging: fact or artifact?** *AJNR Am J Neuroradiol* 2001;22:239–40
3. Cordes D, Haughton VM, Arfanakis K, et al. **Frequencies contributing to functional connectivity in the cerebral cortex in "resting-state" data.** *AJNR Am J Neuroradiol* 2001;22:1326–33
4. Birn RM, Diamon JB, Smith MA, et al. **Separating respiratory-variation-related fluctuations from neuronal-activity-related fluctuations in fMRI.** *Neuroimage* 2006;31:1536–48
5. Grecius MD, Krasnow B, Reiss AL, et al. **Functional connectivity in the resting brain: a network analysis of the default mode hypothesis.** *Proc Natl Acad Sci U S A* 2003;100:253–58
6. Fox MD, Snyder AZ, Vincent JL, et al. **The human brain is intrinsically organized into dynamic, anticorrelated functional networks.** *Proc Natl Acad Sci U S A* 2005;102:9673–78
7. Damoiseaux JS, Rombouts S, Barkhof F, et al. **Consistent resting-state networks across healthy subjects.** *Proc Natl Acad Sci U S A* 2006;103:13848–53
8. Shulman GL, Fiez JA, Corbetta M, et al. **Common blood flow changes across visual tasks: II. Decreases in cerebral cortex.** *J Cog Neurosci* 1997;9:648–63
9. Raichle ME, MacLeod AM, Snyder AZ, et al. **A default mode of brain function.** *Proc Natl Acad Sci U S A* 2001;98:676–82
10. Laufs H, Krakow K, Sterzer P, et al. **Electroencephalographic signatures of attentional and cognitive default modes in spontaneous brain activity fluctuations at rest.** *Proc Natl Acad Sci U S A* 2003;100:11053–58
11. Cordes D, Haughton VM, Arfanakis K, et al. **Mapping functionally related regions of brain with functional connectivity MR imaging.** *AJNR Am J Neuroradiol* 2000;21:1636–44
12. Wang K, Jiang T, Yu C, et al. **Spontaneous activity associated with primary visual cortex: a resting-state fMRI study.** *Cereb Cortex* 2008;18:697–704
13. Vincent JL, Snyder AZ, Fox MD, et al. **Coherent spontaneous activity identifies a hippocampal-parietal memory network.** *J Neurophysiol* 2006;96:3517–31
14. Stein T, Moritz C, Quigley M, et al. **Functional connectivity in the thalamus and hippocampus studied with functional MR imaging.** *AJNR Am J Neuroradiol* 2000;21:1397–401
15. Salvador R, Suckling J, Coleman MR, et al. **Neurophyiological architecture of functional magnetic resonance images of human brain.** *Cereb Cortex* 2005;15:1332–42. Epub 2005 Jan 5
16. Mukamel R, Gelbard H, Arieli A, et al. **Coupling between neuronal firing, field potentials, and fMRI in human auditory cortex.** *Science* 2005;309:951–54
17. Xu G, Xu Y, Wu G, et al. **Task-modulation of functional synchrony between spontaneous low-frequency oscillations in the human brain detected by fMRI.** *Mag Reson Med* 2006;56:41–50
18. Fox MD, Snyder AZ, Zacks JM, et al. **Coherent spontaneous activity accounts for trial-to-trial variability in human evoked brain responses.** *Nat Neurosci* 2006;9:23–25
19. Yang H, Long XY, Yang Y, et al. **Amplitude of low frequency fluctuation within visual areas revealed by resting-state functional MRI.** *Neuroimage* 2007;36:144–52
20. Turner KC, Frost L, Linsenbardt D, et al. **Atypically diffuse functional connectivity between caudate nuclei and cerebral cortex in autism.** *Behav Brain Func* 2006;2:34
21. Villalobos ME, Mizuno A, Dahl BC, et al. **Reduced functional connectivity between V1 and inferior frontal cortex associated with visuomotor performance in autism.** *Neuroimage* 2005;25:916–25
22. Grecius MD, Srivastava G, Reiss AL, et al. **Default-mode network activity distinguishes Alzheimer's disease from healthy aging: evidence from functional MRI.** *Proc Natl Acad Sci U S A* 2004;101:4637–42
23. Bokde ALW, Lopez-Bayo P, Meindl T, et al. **Functional connectivity of the fusiform gyrus during a face-matching task in subjects with mild cognitive impairment.** *Brain* 2006;129:1113–24
24. Lowe MJ, Phillips MD, Lurito JT, et al. **Multiple sclerosis: low-frequency temporal blood oxygen level-dependent fluctuations indicate reduced functional connectivity: initial results.** *Radiology* 2002;224:184–92

25. Liu Y, Yu C, Liang M, et al. **Whole brain functional connectivity in the early blind.** *Brain* 2007;130:2085–96
26. Liang M, Zhou Y, Jiang T, et al. **Widespread functional disconnectivity in schizophrenia with resting-state functional magnetic resonance imaging.** *Neuroreport* 2006;17:209–13
27. Quigley M, Cordes D, Turski P, et al. **Role of the corpus callosum in functional connectivity.** *AJNR Am J Neuroradiol* 2003;24:208–12
28. Lowe MJ, Dzemidzic M, Lurito JT, et al. **Correlations in low-frequency BOLD fluctuations reflect cortico-cortical connections.** *Neuroimage* 2000;12:582–87
29. Brainard DH. **The psychophysics toolbox.** *Spat Vis* 1997;10:433–36
30. Brett M, Anton J-L, Valabregue R, et al. **Region of interest analysis using an SPM toolbox [abstract]: 8th International Conference on Functional Mapping of the Human Brain** [on CD-ROM]. *Neuroimage* 2002;16
31. Leopold DA, Murayama Y, Logothetis NK. **Very slow activity fluctuations in monkey visual cortex: implications for functional brain imaging.** *Cereb Cortex* 2003;13:422–33
32. Niessing J, Ebisch B, Schmidt KE, et al. **Hemodynamic signals correlate tightly with synchronized gamma oscillations.** *Science* 2005;309:948–51
33. Nir Y, Fisch L, Mukamel R, et al. **Coupling between neuronal firing rate, gamma LFP, and BOLD fMRI is related to interneuronal correlations.** *Curr Biol* 2007;17:1275–85
34. Mantini D, Perrucci MG, Del Gratta C, et al. **Electrophysiological signatures of resting state networks in the human brain.** *Proc Natl Acad Sci U S A* 2007;104:13170–75
35. Lu H, Zuo Y, Gu H, et al. **Synchronized delta oscillations correlate with the resting-state functional MRI signal.** *Proc Natl Acad Sci U S A* 2007; 104:18265–69
36. Canolty RT, Edwards E, Dalal SS, et al. **High gamma power is phase-locked to theta oscillations in human neocortex.** *Science* 2006;313:1626–28
37. Beggs JM, Plenz D. **Neuronal avalanches in neocortical circuits.** *J Neurosci* 2003;23:11167–77
38. Wilson CJ, Kawaguchi Y. **The origins of two-state spontaneous membrane potential fluctuations of neostriatal spiny neurons.** *J Neurosci* 1996; 16:2397–410
39. Anderson J, Lampl I, Reichova I, et al. **Stimulus dependence of two-state fluctuations of membrane potential in cat visual cortex.** *Nat Neurosci* 2000; 3:617–21
40. Lampl I, Reichova I, Ferster D. **Synchronous membrane potential fluctuations in neurons of the cat visual cortex.** *Neuron* 1999;22:361–74
41. Destexhe A, Contreras D. **Neuronal computation with stochastic network states.** *Science* 2006;314:85–90
42. Christensen K, Olami Z, Bak P. **Deterministic 1/f noise in nonconservative models of self-organized criticality.** *Phys Rev Lett* 1992;68:2417–20
43. Maxim V, Sendur L, Fadili J, et al. **Fractional Gaussian noise, functional MRI, and Alzheimer's disease.** *Neuroimage* 2005;25:141–58